Chemical Shift Parameters and Molecular Motion in Poly(butylene terephthalate) and Poly(butylene terephthalate)-Containing Polymers

Lynn W. Jelinski

Bell Laboratories, Murray Hill, New Jersey 07974. *Received March 9, 1981*

ABSTRACT: ^{13}C NMR chemical shift tensor parameters are obtained for model compounds and for polymers containing poly(butylene terephthalate) by using the Herzfeld–Berger method. The model compounds are glycine, hexamethylbenzene, and dimethyl terephthalate; the polymers are poly(butylene terephthalate) and two segmented copolymers of poly(butylene terephthalate) plus poly(butylene ether) glycol, containing 0.04 and 0.20 mole fraction of "soft" butylene ether segments. The $OCH_2CH_2CH_2CH_2O$ carbons in poly(butylene terephthalate) move between lattice positions at a rate which is fast compared to the methylene chemical shift interaction ($\bar{\tau} < 10^{-3}$ s). The carbonyl carbon chemical shift tensor is axially symmetric for dimethyl terephthalate and for the three polymer samples. The full width ($|\sigma_{33} - \sigma_{11}|$) of the protonated aromatic carbon chemical shift anisotropy for the "softest" segmented copolymer is less than that of the other samples. This narrowing is attributed to molecular motions of the aromatic rings which are fast compared to the chemical shift anisotropy. The effects of motional heterogeneity and the sources of errors in this method are discussed.

Introduction

We report here the first application of reconstructed ^{13}C chemical shift anisotropies to characterize molecular motion in polymers. High-resolution solid-state ^{13}C NMR has become a routine technique and recent reviews have described both solid-state NMR[1,2] and its application for the study of polymers.[3-5] Therefore, we will describe only briefly the techniques we have employed. When the static dipolar interaction is removed by high-power irradiation of the protons at their Larmor frequency,[1,6,7] the residual line shape is determined primarily by the chemical shift anisotropy. The chemical shift anisotropy or the motionally narrowed line shape can give information concerning both the rate and angular range of molecular reorientation.[1,8] In addition to dipolar decoupling, Hartmann–Hahn matched cross polarization[7] can be used to circumvent the long carbon T_1 values normally found in solids. ^1H–^{13}C cross polarization markedly reduces the time required to accumulate solid-state spectra and provides a fourfold sensitivity enhancement.[7] Magic angle spinning[9] (MAS) can be used in conjunction with dipolar decoupling[10] and cross polarization to remove the chemical shift anisotropy and reveal the isotropic chemical shifts. MAS is particularly useful if the static spectrum is composed of overlapping chemical shift anisotropy powder patterns. If the rotation rate is less than the chemical shift anisotropy, the powder pattern will contain sidebands dispersed about the isotropic chemical shift.[11,12]

Although MAS provides isotropic chemical shift values, this increase in resolution is at the expense of the information contained in the chemical shift anisotropy.[8] Several techniques have been proposed to regain the chemical shift anisotropy information. Among these are slow-spinning magic angle ^{13}C NMR,[8] fast spinning about an axis slightly displaced from the magic angle,[8] half-revolution-synchronized 180° ^{13}C radio-frequency pulses,[13] and moment analysis of the sidebands.[14] Each of these methods has been used with various degrees of success. Recognizing that the individual spinning sideband intensities are complicated functions of the chemical shift parameters,[13,14] Herzfeld and Berger developed expressions for the sideband intensities and evaluated them numerically.[15] They constructed graphical and numerical methods for extracting the chemical shift parameters from the intensities of just a few sidebands.[15] The Herzfeld–Berger method is particularly powerful if one is unable to measure accurately all of the sidebands, as is often the case when aromatic and aliphatic residues are present in the same molecule.

We begin our discussion by illustrating that the aliphatic region of the ^{13}C NMR powder spectrum of poly(butylene terephthalate) provides direct evidence for molecular motion in the polymer. The carbonyl/aromatic region of the spectrum, on the other hand, contains little direct information, as this portion of the spectrum is composed of overlapping resonances from three types of carbons. Therefore we obtain the chemical shift parameters for this region of the spectrum from a Herzfeld–Berger analysis[15] of the intensities of the magic angle spinning sidebands. We first use model compounds to establish the validity of the Herzfeld–Berger method and then obtain the chemical shift parameters for poly(butylene terephthalate) and related compounds. We then consider the possibility of motional heterogeneity and its effect on the sideband intensity analysis. Finally, we discuss the errors which result from this type of analysis and assess the capability of this method to provide sufficiently accurate motional information.

Experimental Section

Dimethyl terephthalate (I) and poly(butylene terephthalate) (II) were obtained from Eastman Chemical Co. The poly(butylene

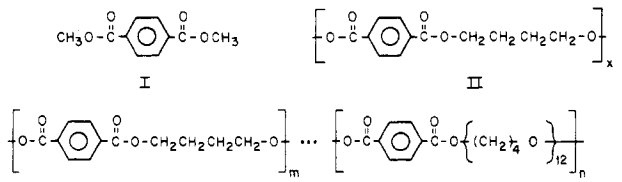

I II

III m/n = 24

IV m/n = 4

terephthalate) sample has $\bar{M}_w$ = 33 500 and a T_g of 80 °C. High-resolution solution-state NMR characterization showed no resonances due to end groups. Glycine and hexamethylbenzene were from Aldrich Chemical Co. The segmented copolymers III and IV were kindly provided by du Pont Co. The ratios of "hard" to "soft" segments and the average hard block length of these copolymers have been determined previously.[16] Polymer samples in the form of powder or pellets were packed into machined Kel-F rotors by hand or by a nonhydraulic pellet press. The volume of the sample rotors is 0.3 cm^3.

Solid-state ^{13}C NMR spectra were recorded at 47 kG (50.3 MHz for ^{13}C) on a Varian XL-200 spectrometer equipped with an

0024-9297/81/2214-1341$01.25/0

Table I
Chemical Shift Parameters for Poly(butylene terephthalate) and Related Compounds[a]

sample	ω_{rot}, kHz	carbonyl carbon $\lvert\sigma_{33}-\sigma_{11}\rvert$,[b] ppm	carbonyl carbon ρ[c]	nonprotonated aromatic $\lvert\sigma_{33}-\sigma_{11}\rvert$,[b] ppm	nonprotonated aromatic ρ[c]	protonated aromatic $\lvert\sigma_{33}-\sigma_{11}\rvert$,[b] ppm	protonated aromatic ρ[c]
glycine	2.19	144 ± 4[d]	−0.023 ± 0.03[e]				
glycine	1.70	140 ± 4[d]	−0.028 ± 0.03[e]				
hexamethylbenzene	2.80			171 ± 4[f]	−1.0 ± 0.1[g]		
I	2.21	137 ± 4	+1.0 ± 0.1	201 ± 4	−0.24 ± 0.02	215 ± 4	−0.38 ± 0.03
II	1.14	127 ± 5	+1.0 ± 0.1	202 ± 5	−0.20 ± 0.03	198 ± 5	−0.39 ± 0.02
III	2.34	133 ± 7	+1.0 ± 0.1	198 ± 7	−0.23 ± 0.07	201 ± 4	−0.32 ± 0.02
III	2.18	130 ± 4	+1.0 ± 0.1	199 ± 5	−0.15 ± 0.07	196 ± 3	−0.40 ± 0.01
IV	2.05	132 ± 3	+1.0 ± 0.1	203 ± 5	−0.25 ± 0.05	187 ± 3	−0.40 ± 0.02

[a] Chemical shift parameters were obtained from the ratios of spinning sideband intensities by the method of Herzfeld and Berger;[15] each value represents the average of at least two independent measurements. [b] $\lvert\sigma_{33}-\sigma_{11}\rvert = \mu\omega_{rot}/\gamma H_0$. [c] $\rho = (\sigma_{11}+\sigma_{33}-2\sigma_{22})/(\sigma_{33}-\sigma_{11})$; $\sigma_{33} > \sigma_{22} > \sigma_{11}$. [d] Literature values:[32,33] 144.6, 144.7, 142.2 ppm. [e] Literature values:[32,33] −0.051, −0.089, 0.00. [f] Literature value:[22,35] 168 ppm. [g] Literature value:[22,35] −1.0.

auxiliary high-power amplifier and a solid-state probe with magic angle spinning capability. The strength of the high-power proton decoupling field was ~45 kHz (12 G). The Hartmann–Hahn condition[17] and the magic angle were adjusted by using the aromatic signal from hexamethylbenzene. Probe tuning was optimized and the reflected power from the decoupler was minimized for each sample. All spectra were obtained at ambient temperature and in the unlocked mode (estimated drift <0.01 ppm/h). The static spectra were recorded in a 40-kHz spectral window with 2K time-domain data points; the spectra with magic angle sample spinning were obtained in a 20-kHz spectral window with 4K time-domain data points. The proton-enhanced spectra were obtained by using proton spin temperature alternation.[18] The free induction decays were zero-filled prior to transformation. The number of accumulations, the repetition rate, and the cross polarization contact time for each spectrum are listed in the figure legends.

Peak heights measured directly from the spectra were used in the chemical shift anisotropy reconstructions.[15] The principal elements of the chemical shift tensors were determined by graphical interpolation of data in ref 15; error estimates were made from the dispersion in the intersection of the μ and ρ values, according to the methods outlined in ref 15. Each value in Table I represents the average of at least two determinations. We have found that at our 47-kG field strength, a ~2-kHz spinning rate provides the best compromise between minimization of noise[14] and optimization of the number of measurable sidebands for carbonyl and aromatic carbons. The optimum amount of line broadening was found to be 20 Hz.

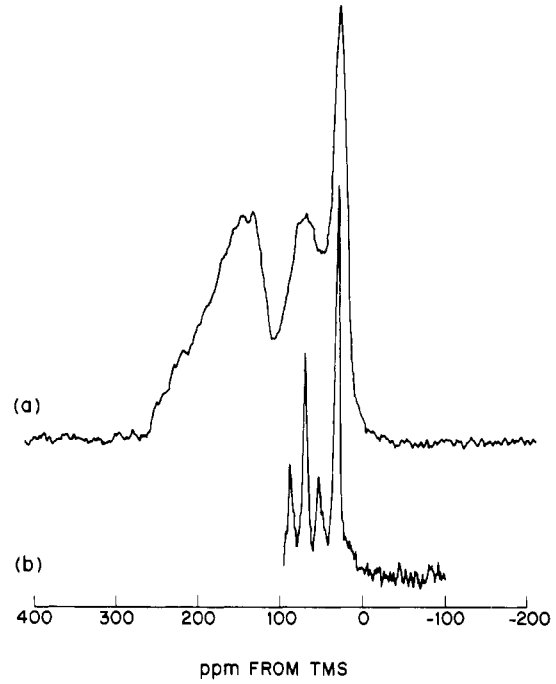

Figure 1. Proton-enhanced, dipolar-decoupled 50.3-MHz ^{13}C NMR spectra of 0.3 g of poly(butylene terephthalate): (a) static powder spectrum (8192 accumulations, 3-s repetition rate, 0.5-ms contact time); (b) aliphatic region of sample in (a) (MAS at 0.88 kHz, 4069 accumulations, 1-s repetition rate, 0.3-ms contact time).

Results and Discussion

The proton-enhanced static ^{13}C NMR powder spectrum of poly(butylene terephthalate) (II) (Figure 1a) consists of a sharp resonance centered at 29 ppm which arises from the CH_2 carbons flanked by CH_2 carbons on either side. The broader resonance centered at ca. 70 ppm arises from the OCH_2 carbons, and the peak extending from ca. 250 ppm upfield into the aliphatic region is due to the overlapping chemical shift anisotropy powder patterns from the carbonyl, protonated aromatic, and nonprotonated aromatic carbons. The 29- and 70-ppm resonances differ threefold in width. Slow-speed magic angle spinning (MAS) can be used to determine whether the breadth of the OCH_2 resonance at ca. 70 ppm is due to motional broadening phenomena[1,19,20] or whether it reflects an inherent difference in chemical shift anisotropy.[21] In the ^{13}C NMR spectrum of poly(butylene terephthalate) obtained with MAS at 0.88 kHz (Figure 1b), the OCH_2 carbon signal at ca. 70 ppm is flanked by intense sidebands, whereas the $OCH_2CH_2CH_2CH_2O$ signal at 29 ppm is not. This result establishes that the chemical shift anisotropies for these two types of carbons are very different at ambient temperature. We estimate that the OCH_2 carbon anisotropy ($\lvert\sigma_{33}-\sigma_{11}\rvert$) for poly(butylene terephthalate) at ambient temperature is ca. 60 ppm, a value which is in agreement with rigid lattice anisotropies reported for other OCH_2 carbons (57 ppm for ethanol at −170 °C[22] and 79 ppm for diethyl ether at −140 °C[22]). However, the ca. 14-ppm anisotropy which we observe for the $OCH_2CH_2CH_2CH_2O$ carbons of poly(butylene terephthalate) is significantly smaller than the rigid lattice anisotropies which have been observed for other alkane methylene carbons (viz., 33 ppm for the internal CH_2 carbons of *n*-eicosane at −95 °C[23] and 38 ppm for amorphous linear polyethylene[24]). This observation suggests that, at ambient temperature, the chemical shift anisotropy for the $OCH_2CH_2CH_2CH_2O$ carbons of poly(butylene terephthalate) has been partially averaged by molecular motion. This result is corroborated by the short T_1 value (ca. 0.3 s) observed for these carbons.[25] In addition, this result is consistent with the high degree of disorder found by X-ray fiber diffraction studies of this polymer.[26,27] These NMR results indicate that the central CH_2 carbons in poly(butylene terephthalate) undergo motions which do not involve the OCH_2 carbons to a great extent.

X-ray fiber diffraction studies show that the fiber repeat distance for this polymer is less than expected, when compared to the results of other linear aromatic esters.[26,27] Shortening of the expected fiber repeat distance has been localized in the OCH_2CH_2 part of the chain[26] and requires that the chain conformation be kinked.[27] An approximately gauche–trans–gauche conformation for the alkyl portion of unstressed poly(butylene terephthalate) has been advanced to explain the X-ray diffraction results.[28] These solid-state ^{13}C NMR results are consistent with a model in which the central $-CH_2-$ carbons undergo torsional oscillations within the gauche–trans–gauche conformational energy well. The rate of this motion is fast compared to the chemical shift interaction ($\tau_c < 10^{-3}$ s).

In view of the molecular motion of the poly(butylene terephthalate) $OCH_2CH_2CH_2CH_2O$ carbons suggested by the static powder pattern, it was of interest to investigate further the chemical shift parameters of the carbonyl and aromatic carbons in a series of related compounds. These included crystalline dimethyl terephthalate (I) (the "rigid" case), poly(butylene terephthalate) (II), and two segmented copolymers, III and IV, which contain lamellar networks of poly(butylene terephthalate) "hard" segments.[29] Wide-angle X-ray diffraction patterns of the drawn segmented copolymers III and IV are identical with the patterns for the homopolymer poly(butylene terephthalate) (II), with the exception of a halo due to amorphous material in the former polymers.[29] This result has been taken to indicate that the poly(butylene terephthalate) segments in both the copolymer and the homopolymer crystallize in the same way.[29]

That the broad featureless carbonyl/aromatic resonances shown for poly(butylene terephthalate) (Figure 1a) and for the segmented copolymer III (Figure 2a) are composed of three partially overlapping chemical shift tensor powder patterns with different isotropic chemical shifts and different anisotropies can be observed by inspection of Figure 2b. Discrimination among sidebands and isotropic resonances can be performed by multiplying together two spectra obtained at different spinning speeds, by visual inspection, or by a combination of these techniques. Sideband identification is straightforward for this relatively simple polymer spectrum; the results are shown in Figure 2c. The peaks can be assigned by comparision with the solution spectrum (Figure 2d) and by comparison with the chemical shifts for similar polymers.[30,31] In increasing upfield order, the peaks are assigned to the carbonyl carbons, the nonprotonated aromatic carbons, the protonated aromatic carbons, OCH_2 carbons from the "soft" poly(butylene ether) segments, the OCH_2 carbons from the poly(butylene terephthalate) "hard" segments, and overlapping resonances of the $OCH_2CH_2CH_2CH_2O$ carbons from both the "hard" and "soft" segments.

Sets of spectra similar to Figure 2 were obtained for two model compounds (glycine and hexamethylbenzene) and for samples I–IV. The intensities of the sidebands from MAS were used to obtain the chemical shift parameters by the Herzfeld–Berger method.[15] Herzfeld and Berger have defined two parameters, μ and ρ, which are related to the chemical shift tensor elements σ_{11}, σ_{22}, and σ_{33} by[15]

$$\mu = \frac{\gamma H_0(\sigma_{33} - \sigma_{11})}{\omega_{rot}} \quad (1)$$

$$\rho = \frac{\sigma_{11} + \sigma_{33} - 2\sigma_{22}}{\sigma_{33} - \sigma_{11}} \quad (2)$$

Here, $\sigma_{33} > \sigma_{22} > \sigma_{11}$, γ is the gyromagnetic ratio of the nucleus under observation, H_0 is the magnetic field strength, and ω_{rot} is the rotor speed. Relative sideband-to-centerband intensities for $\pm i$ (high and low frequency) sidebands have been plotted as functions of μ and ρ.[15] These plots appears as "contour maps", with a separate plot for each high- and low-frequency sideband. Each contour on the plots corresponds to a specific value of the ratio of the $\pm i$th sideband compared to the centerband.

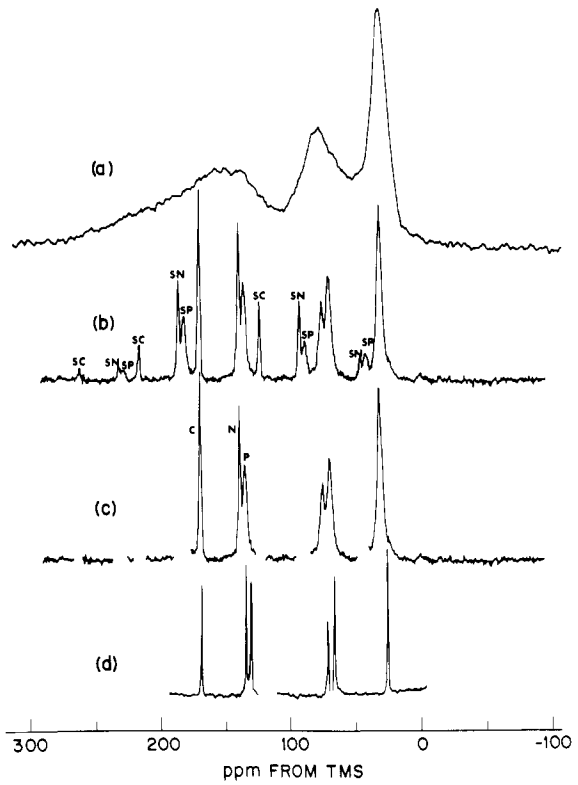

Figure 2. ^{13}C NMR spectra (50.3 MHz) of segmented copolymer III: (a) static powder pattern obtained by cross polarization and dipolar decoupling (0.3 g sample, 8192 accumulations, 0.5-ms contact time, 3-s repetition rate); (b) proton-enhanced, dipolar-decoupled spectrum of sample in (a) (MAS at 2.3 kHz, 1024 accumulations, 1-ms contact time, 3-s repetition rate); (c) spectrum in (b) in which the sidebands have been removed; (d) Overhauser-suppressed, proton-decoupled spectrum of 21 wt % solution of the polymer in hexafluoroisopropyl alcohol (512 accumulations, 10-s repetition rate, 34 °C). The solvent peaks have been removed and the lines have been artifically broadened. The carbonyl, C, nonprotonated aromatic, N, and protonated aromatic, P, carbon resonances are assigned in (c), and the respective sidebands are designated with the prefix S in (b). For example, a peak marked SC is a sideband of the carbonyl carbon line.

One measures from the experimental NMR spectrum as many of the sideband intensities as are clearly resolved. The ratios of these sideband-to-centerband intensities are then calculated. One prepares a composite graph of the contours which correspond to the intensity ratios for each $\pm i$th sideband. Two examples of such composite graphs are shown in Figure 3. The parameters μ and ρ are then read from the point where the contour lines from all of the high- and low-frequency sidebands intersect (see Figure 3). The chemical shift parameters are obtained by solving three simultaneous linear equations (eq 1 and 2, above, and $\sigma_i = (\sigma_{11} + \sigma_{22} + \sigma_{33})/3$). The degree of dispersion in the intersection of the lines provides an estimate of the uncertainty in μ and ρ.[15]

The results of spinning sideband reconstruction of the chemical shift parameters for the carbonyl and aromatic carbons of model compounds and polymers II–IV are listed in Table I. The first two entries in Table I illustrate the reconstruction of an anisotropy whose principal values

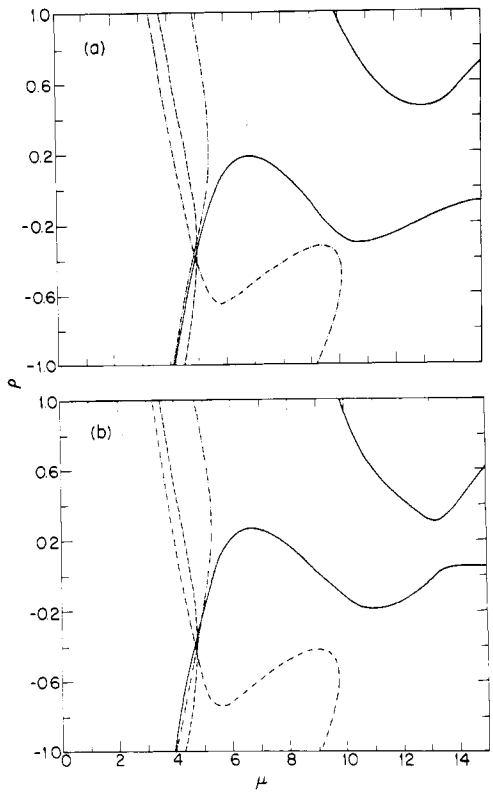

Figure 3. Representative contour plots used to obtain the chemical shift parameters: (a) protonated aromatic carbons of dimethyl terephthalate; (b) protonated aromatic carbons of segmented copolymer IV. In these plots (– – –) and (· · ·) correspond to the respective low- and high-frequency second sidebands; (—) and (– · –) correspond to the low- and high-frequency first sidebands, respectively.

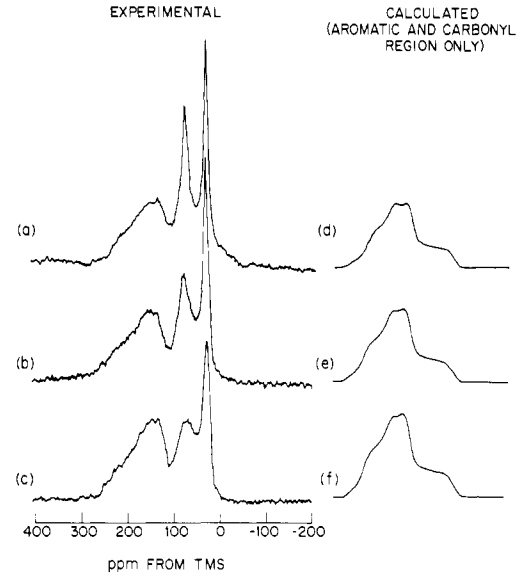

Figure 4. Comparison of experimental (a–c) and calculated[1] (d–f) solid-state ^{13}C NMR spectra for (a) segmented copolymer IV, (b) polymer III, and (c) poly(butylene terephthalate) (II). The calculated spectra represent the carbonyl and aromatic regions only. The spectra were calculated by summing the individual carbonyl, nonprotonated aromatic, and protonated aromatic powder patterns (with the proper weighting), using the values from Table I.

have been determined by single-crystal studies.[32,33] The literature and experimental values for the carbonyl carbon of glycine are in good agreement. The next entry in Table I illustrates the reconstruction of the nonprotonated aromatic carbon anisotropy for hexamethylbenzene. At ambient temperatures, hexamethylbenzene undergoes rapid sixfold jump diffusion about the hexad axis.[1,22,34] The literature[22,35] and experimental values are in good agreement for this motionally narrowed anisotropy. Having established the validity of the Herzfeld–Berger method[15] for recovery of the chemical shift parameters in simple model compounds, we now apply this method to systems which contain overlapping carbonyl and aromatic resonances.

Dimethyl terephthalate (I) is a highly crystalline material in which the aromatic ring occupies a rigid lattice position.[32] The carbonyl carbon chemical shift powder pattern for I is axially symmetric, as are the carbonyl carbon anisotropies for the terephthalate-containing polymers II–IV (Table I) (i.e., $\rho = +1.0$). Polymers II–IV contain somewhat reduced carbonyl carbon anisotropies; however, the experimental error is such that this apparent trend may not be significant.

The full chemical shift anisotropies for the nonprotonated aromatic carbons of dimethyl terephthalate and for polymers II–IV are very similar and are in line with the full anisotropies for other nonprotonated aromatic carbons.[1,22] The protonated aromatic carbon anisotropy for dimethyl terephthalate (I), although similar to reported values,[22] is significantly larger than for the terephthalate-containing polymers II–IV. Whether this difference is due to an inherent difference in anisotropies or is caused by molecular motion in the polymers is uncertain at this time. There is also a significant decrease in the chemical shift anisotropy in going from segmented polymer III (which contains very little "soft" segment) to polymer IV (which contains six times more "soft" segment). We believe that this difference does reflect increased molecular motion of the phenyl rings in the softer of the two segmented polymers. This result is supported by the different T_1 values observed for the protonated aromatic carbons for the two polymers (~3 s for III and ~0.25 s for IV)[25] and by experiments involving scalar, rather than dipolar, decoupling.[16,37] Scalar-decoupled static and magic angle spinning experiments indicate that the motions of the phenyl groups in the copolymer IV are sufficiently rapid to partially average the ^1H–^{13}C dipolar interaction of the protonated aromatic carbons.[16,37] The torsional angles and the extent of the phenyl group motion are currently under consideration. However, significant motions do not appear to occur only in the plane of the aromatic rings. The most shielded components of aromatic chemical shift tensors have directions perpendicular to the aromatic rings[1,38] and are thus common to both the protonated and nonprotonated carbons. If significant in-plane motions were the only ones present, we would expect the chemical shift anisotropies for both types of aromatic carbons to be affected equally. This is not the case (Table I). Rather, the aromatic ring motions probably involve small-angle excursions about the 1,4-phenylene axis.

The chemical shift powder patterns for polymers II–IV were calculated[1] with the chemical shift parameters listed in Table I. Figure 4 compares the experimental powder patterns with the calculated carbonyl and aromatic regions. The experimental and calculated spectra are in excellent agreement.

A complication arises in copolymer systems such as III and IV in that aromatic groups in different regions of the polymers may undergo motions which are different. The reconstructed chemical shift parameters then reflect weighted averages of perhaps two or more anisotropies which have been averaged by different amounts. Large errors, particularly in the second and higher order side-

bands, are expected. Small errors of this type were observed, particularly for copolymer III. (It should be noted that the higher order sidebands are also subject to large errors in measured intensity.) The chemical shift parameters which have been reconstructed for the same polymer at different spinning speeds are expected to be identical if the motions of the group under consideration are uniform. The entries in Table I for compound III indicate that the data are not significantly different to indicate motional heterogenity, within the error limits.

A limitation of this method for obtaining chemical shift parameters lies in the accuracy with which one is able to measure the relative intensities of the MAS sidebands. This accuracy is related to the ability to define unambiguously the base line. The base line is clearly resolved in MAS spectra for model systems such as the carbonyl carbon of glycine or the phosphorus in barium diethyl phosphate,[15] as the corresponding static powder spectra are composed of a single resonance. The polymers studied here and most other materials of interest have static powder spectra which are composed of overlapping resonances. It is for these materials (i.e., compounds for which the chemical shift parameters cannot be measured directly from the powder spectra) that chemical shift parameter recovery affords the greatest potential for information. However, upon MAS these overlapping chemical shift patterns often reduce to a complex pattern of lines which may not all be resolved to the base line and which may reflect different line widths (see Figure 2b, for example). The problem of base line definition is probably the largest source of error.

In summary, we have illustrated that reconstructed chemical shift parameters can be used to deduce motional information in polymers. The transition from the qualitative motional information reported here to quantitative information concerning torsional oscillations has several requirements. First, one must be able to distinguish between motional dispersion and motional homogeneity. Second, one must be able to reconstruct the chemical shift parameters from spectra obtained with MAS at very low temperatures. Finally, data acquisition and data manipulation techniques must be optimized, as it is clear that the accuracy of the motional information available from reconstruction of chemical shift anisotropies relies upon the ability to measure with precision the magic angle spinning sideband intensities. We are currently involved in work along these lines.

Acknowledgment. The author is grateful to Drs. D. L. VanderHart, R. G. Griffin, and A. J. Vega for helpful discussions and to Drs. J. Herzfeld and A. E. Berger for furnishing us with a copy of their manuscript prior to publication.

References and Notes

(1) Mehring, M. In "NMR—Basic Principles and Progress"; Diehl, P., Fluck, E., Kosfeld, R.; Eds.; Springer-Verlag: New York, 1976.
(2) Griffin, R. G. *Anal. Chem.* **1977**, *49*, 951.
(3) Lyerla, J. R., Jr. In "Contemporary Topics in Polymer Science"; Shen, M., Ed.; Plenum: New York, 1979; pp 143–213.
(4) Schaefer, J.; Stejskal, E. O. In "Topics in Carbon-13 NMR Spectroscopy"; Levy, G. C., Ed.; Wiley: New York, 1979; Vol. 3, pp 283–324.
(5) McBrierty, V. J.; Douglass, D. C. *Phys. Rep.* **1980**, *63*, 61.
(6) Bloch, F. *Phys. Rev.* **1958**, *111*, 841.
(7) Pines, A.; Gibby, M. G.; Waugh, J. S. *J. Chem. Phys.* **1973**, *59*, 569.
(8) Stejskal, E. O.; Schaefer, J.; McKay, R. A. *J. Magn. Reson.* **1977**, *25*, 569.
(9) Andrew, E. R. *Prog. NMR Spectrosc.* **1972**, *8*, 1.
(10) Schaefer, J.; Stejskal, E. O. *J. Am. Chem. Soc.* **1976**, *98*, 1031.
(11) Waugh, J. S.; Maricq, M. M.; Cantor, R. *J. Magn. Reson.* **1978**, *29*, 183.
(12) Maricq, M.; Waugh, J. S. *Chem. Phys. Lett.* **1977**, *47*, 327.
(13) Lippmaa, E.; Alla, M.; Tuherm, T. In "Magnetic Resonance and Related Phenomena" (Proceedings of the XIXth Congress Ampère); Groupment Ampère: Heidelberg, 1976; pp 113–118.
(14) Maricq, M. M.; Waugh, J. S. *J. Chem. Phys.* **1979**, *70*, 3300.
(15) Herzfeld, J.; Berger, A. E. *J. Chem. Phys.* **1980**, *73*, 6021.
(16) Jelinski, L. W.; Schilling, F. C.; Bovey, F. A. *Macromolecules* **1981**, *14*, 581.
(17) Hartmann, S. R.; Hahn, E. L. *Phys. Rev.* **1962**, *128*, 2042.
(18) Stejskal, E. O.; Schaefer, J. *J. Magn. Reson.* **1975**, *18*, 560.
(19) Fyfe, C. A.; Lyerla, J. R.; Volksen, W.; Yannoni, C. S. *Macromolecules* **1979**, *12*, 757.
(20) Jelinski, L. W.; Torchia, D. A. *J. Mol. Biol.* **1979**, *133*, 45.
(21) Rothwell, W. P.; Waugh, J. S.; Yesinowski, J. P. *J. Am. Chem. Soc.* **1980**, *102*, 2637.
(22) Pines, A.; Gibby, M. G.; Waugh, J. S. *Chem. Phys. Lett.* **1972**, *15*, 373.
(23) VanderHart, D. L. *J. Chem. Phys.* **1976**, *64*, 830.
(24) Urbino, J.; Waugh, J. S. *Proc. Natl. Acad. Sci. U.S.A.* **1974**, *71*, 5062.
(25) Jelinski, L. W.; Dumais, J. J. *Polym. Prepr., Am. Chem. Soc., Div. Polym. Chem.* **1981**, *22* (2), 273.
(26) Mencik, Z. *J. Polym. Sci., Polym. Phys. Ed.* **1975**, *13*, 2173.
(27) Alter, U.; Bonart, R. *Colloid Polym. Sci.* **1976**, *254*, 348.
(28) Stach, W.; Holland-Moritz, K. *J. Mol. Struct.* **1980**, *60*, 49 and references cited.
(29) Cella, R. J. *Encycl. Polym. Sci. Technol.* **1977**, *Suppl. V2*, 485.
(30) Komoroski, R. A. *J. Polym. Sci., Polym. Phys. Ed.* **1979**, *17*, 45.
(31) Kricheldorf, H. R. *Makromol. Chem.* **1978**, *179*, 2133.
(32) Griffin, R. G.; Pines, A.; Waugh, J. S. *J. Chem. Phys.* **1975**, *63*, 3676.
(33) Haberkorn, R. A.; Stark, R. E.; van Willigen, H.; Griffin, R. G. *J. Am. Chem. Soc.* **1981**, *103*, 2534.
(34) Tang, J.; Sterna, L; Pines A. *J. Magn. Reson.* **1980**, *41*, 389.
(35) Pausak, S.; Tegenfeldt, J.; Waugh, J. S. *J. Chem. Phys.* **1974**, *61*, 1338.
(36) Alla, M.; Eckman, R.; Pines, A. *Chem. Phys. Lett.* **1980**, *71*, 148.
(37) Bovey, F. A.; Cais, R. E.; Jelinski, L. W.; Schilling, F. C.; Starnes, W. H., Jr.; Tonelli, A. E. *Polym. Prepr., Am. Chem. Soc., Div. Polym. Chem.* **1981**, *22* (1), 268.
(38) Pausak, S.; Pines, A.; Waugh, J. S. *J. Chem. Phys.* **1973**, *59*, 591.